JAES | JOURNAL OF APPLIED ENGINEERING SCIENCE | www.engineeringscience.rs
ISTRAŽIVANJA I PROJEKTOVANJA ZA PRIVREDU

Indexed by

PERFORMANCE EVALUATION ON THE DESIGNED V-SHAPED MONOHULL SHIP MODELS

Aditya Rio Prabowo
Department of Mechanical Engineering, Universitas Sebelas Maret, Surakarta, Indonesia

Rizky Adhi Febrianto
Department of Mechanical Engineering, Universitas Sebelas Maret, Surakarta, Indonesia

Tuswan Tuswan
Department of Naval Architecture, Diponegoro University, Semarang, Indonesia

Dominicus Danardono Dwi Prija Tjahjana
Department of Mechanical Engineering, Universitas Sebelas Maret, Surakarta, Indonesia

Key words: *high-speed craft, monohull, stability, resistance, seakeeping*
doi:10.5937/jaes0-35481

Cite article:

Rio Prabowo A., Adhi Febrianto R., Tuswan T., Dominicus Danardono Dwi Prija T. (2022) PERFORMANCE EVALUATION ON THE DESIGNED V-SHAPED MONOHULL SHIP MODELS , *Journal of Applied Engineering Science*, 20(2), 610 - 624, DOI:10.5937/ jaes0-35481

Online aceess *of full paper is available at: www.engineeringscience.rs/browse-issues*

Istraživanja i projektovanja za privredu
Journal of Applied Engineering Science

Original Scientific Paper

doi:10.5937/jaes0-35481

Paper number: 20(2022)2, 968, 610-624

PERFORMANCE EVALUATION ON THE DESIGNED V-SHAPED MONOHULL SHIP MODELS

Aditya Rio Prabowo[1,]*, Rizky Adhi Febrianto[1], Tuswan Tuswan[2], Dominicus Danardono Dwi Prija Tjahjana[1]
[1]Department of Mechanical Engineering, Universitas Sebelas Maret, Surakarta, Indonesia
[2]Department of Naval Architecture, Diponegoro University, Semarang, Indonesia

A typical ship must operate in extreme conditions in the open coastal zone. Due to the severe operation at sea, comparative research on the design of the hull shape for optimization purposes will be important, specifically in the resistance and movement aspect. In this regard, an investigation was carried out by varying the total of four V-shaped monohull models from the high-built design as the main subject to compare several hull shape designs at the same displacement to obtain better performance at stability, resistance, and seakeeping criteria. Savitsky formula is used to calculate the hull resistance, and the stability analysis is calculated analytically by comparing the relationship between righting arm and heel angle. Moreover, ship motion is investigated by examining heave and roll response amplitude operator (RAO) and Motion Sickness Incident (MSI) index due to wave height 0.1 m. The most significant feature in this study is resistance since, with limited power, a minimum resistance value is necessary for best outcomes. It can be found that Model I is a superior model in terms of resistance, stability, and seakeeping performance to other models. However, Model III is not recommended since it has high resistance and bad stability and motion performance. From these results, it can be summarized that Model I is selected as the best hull form model.

Key words: high-speed craft, monohull, stability, resistance, seakeeping

INTRODUCTION

Oceans encompass most of the earth's surface, accounting for around 71% of the total [1]. Using sea transportation lines to connect islands is a significant problem in logistics distribution. The ship is one of the most vital modes of sea transportation as a way of connecting islands. There are several advantages to using ships in transportation routes, such as trade, exports and imports, technical advancements, and the ability to create cooperative ties between adjacent nations [2-10]. Because of the increased frequency of marine commerce, global economic growth is rising. Because of its low cost, ocean shipping by ship accounts for over 90% of world trade [11]. With the rapid development of ship operations, International Maritime Organization (IMO) developed a new term called Energy Efficiency Design Index (EEDI) to assess the level of Ship Energy Efficiency Management Plan (SEEMP) and its influence on the greenhouse gas (GHG) impact [12]. Scholars have made many efforts to reduce fuel consumption and greenhouse gas emissions. Modification of hull form in the preliminary and early-stage design is categorized as a potential solution to obtain the optimal hydrodynamic performance aspects, including propulsion, resistance, stability, and seakeeping [13-18]. The shape of the hull underwater will affect the fluid flow characteristics around the ship, representing a drag movement. Ships consume a considerable amount of fuel to provide the necessary propellant force to overcome resistance in their movement. There is always a tendency to enhance hull characteristics in order to minimize resistance during ship operation. Several studies have been conducted in order to reduce the resistance on the ship's hull during operation by altering hull form [19,20], demi-hull configuration [21], and hull-propulsion [22]. High-speed crafts operating in planning modes face a variety of stability-related risks, such as decreased transverse stability with increasing speed [23]. Therefore, investigating the hull shape modification in order to obtain high-level stability performance is a crucial aspect of the planning hull. Besides the parameters of resistance and stability, one of the essential characteristics of a fast vessel is its ability to maintain its position in the water. It is challenging to improve the intrinsic seakeeping performance once it has been designed. Rolling, pitching, and heaving motion responses will have an impact on the comfort and safety of the crew and the items being transported. Other researchers performed a seakeeping analysis to evaluate the comfort and safety of people on board. Among these is the MSI analysis, which looks at the percentage of passengers that become seasick when they board a ship. MSI occurs as a result of the ship's vertical movement, which is generated by a mixture of ship heaving and pitching. Several investigations were carried out for passenger ships [24], catamaran [25], and fast boats [26]. Although many studies have risen considerably, selecting a V-hull shape analyzed at a high Froude number with good performance still requires further study. In this case, comprehensive research is conducted to investigate the hydrodynamic performance, including stability, resistance, ship motion, and comfort index due to modification of high-speed v-shape craft hull form. This type of hull form offers a ship with minimal drag movement and excellent maneuverability and still considers the ship's motion stability to

*aditya@ft.uns.ac.id

improve time performance and effectiveness [27]. Considering the discussed case and research opportunity, this study aims to analyze several hull form shapes at the same displacement with different ship main dimensions to obtain better performance at stability, resistance, and seakeeping criteria. Four different hull form dimensions are designed based on RC boat competition requirements. This study uses the Savitsky formula to calculate the hull resistance in the planning speed range in Froude number (Fr) 0.5 - 1.0. The stability test is calculated analytically by comparing the relationship between righting arm (GZ) and heel angle. Moreover, ship motion is investigated by examining the heave RAO, roll RAO, and MSI index at the same Fr analyzed in three different wave headings, including head sea, beam sea, and bow quartering sea.

THEORETICAL BACKGROUND

Ship stability

The ship in operation requires a high level of ship stability, so understanding the stability calculation is an essential point to provide safety guidelines [28,29]. The fundamental concept of the state of stability is based on the equilibrium condition depending on the relation between the positions of the center of gravity and the center of buoyancy. A stable equilibrium is achieved when the vertical position of gravity (G) is lower than the position of the transverse metacenter (M). In contrast, an unstable equilibrium is caused when the vertical position of G is higher than the position of the transverse metacenter (M). The stability of a vessel depends on KB, BM, KG, and GM, as figured out in Figure 1. When the ship experiences heeling, there will be a change in the part of the ship that is submerged in water. This change is the weight of point B will continue to change according to the heel angle. In addition, the righting lever (GZ) value also varies depending on the change in the heel angle. When the maximum GZ value, the ship will have the maximum value of the enforcement moment forced to return to the upright position. When the GZ value decreases, the ship will not have an enforcement moment and will continue the heeling moment Figure 2. The following calculation of the GZ value can be calculated by using Equation 1. If the ship is tilted at more than 15 degrees is considered to have a large heel angle, then use Equation 2, and the righting moment uses Equation 3 [30].

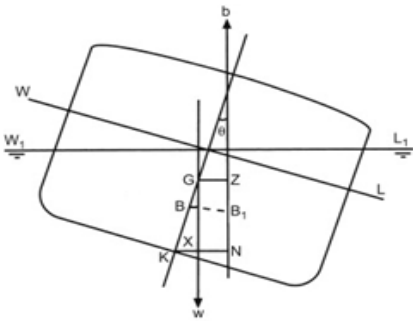

Figure 1: Ship stability point [30]

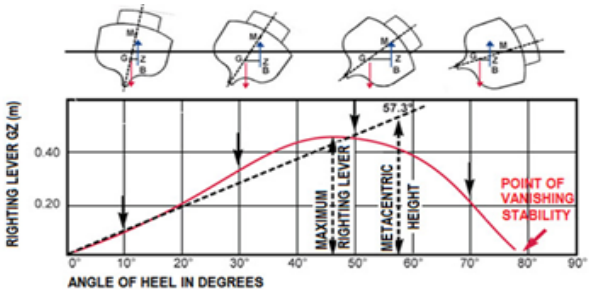

Figure 2: Effect of GZ curve on ship stability [30]

$$GZ = GM\ x\ sin\ \theta \tag{1}$$

$$GZ = (GM + \frac{1}{2} BM \tan^2\theta) \tag{2}$$

$$Righting\ Moment\ (RM) = W\ x\ GZ \tag{3}$$

Where *GZ* is the righting arm, *GM* is the initial metacentric height, W is ship displacement, θ represents heel angle, *BM* is the height of the longitudinal metacenter above the center of buoyancy.

Savitsky resistance method

When the ship is operating, resistance from the fluid passes through the ship hull and will affect the ship's performance [31]. The resistance value gets higher when the ship moves through water and air at a fast-moving speed [32]. The resistance value affects several factors, including ship velocity, wetted surface area, and hull form. The numerical Savitsky method can be used to determine the resistance and power of the planning hull. According to Julianto et al. [32], the Savitsky validation method can be used to estimate the resistance of planning hulls when in the planning mode. According to Savitsky [33], the method is initially researched to measure hydrodynamic design planning of water-based aircraft. However, research is more focused on planning with applications for ships and hydrofoils [33] in further development. The speed coefficient by Savitsky is stated in Equation 4 [33]:

$$C_v = \frac{v}{\sqrt{g.b}} \tag{4}$$

where C_v is the coefficient of speed; *v* is the speed of ship (*m/s*); g is the center of gravity (9.81 m/s^2); b is the maximum beam over chine (m). As for displacement of the designed hull in volume (V^-), it can be calculated using an expression in Equation 5 [33]:

$$\nabla = L\ .B\ .T\ .C_b \tag{5}$$

where, L is the length of waterline (LWL, m); B is the breadth (m); T is the draught (m); C_b is the coefficient of block; V^- is the displacement volume (m^3). Savitsky approaches to find out the value of Reynolds with formulas in Equation 6 [33]:

$$R_n = \frac{V_s . Lwl}{v} \quad (6)$$

where V_s is the service speed (*m/s*); Lwl is the length of waterline (m); v is the viscosity of seawater (m^2/s). C_f is derived using the ITTC formula Equation 7:

$$C_f = \frac{0.075}{(log\ R_n - 2)^2} \quad (7)$$

where, R_n is Reynolds number. The friction component with the Savitsky method can be formulated in the following Equation 8 [33]:

$$D_f = \frac{c_f \rho V^2 (\lambda b^2)}{2 \cos \beta} \quad (8)$$

where D_f is frictional resistance, C_f is a frictional coefficient, ρ is the density of seawater, β is deadrise angle, b is the maximum distance above the chine, λ is the average value of the ratio of length and width in the wet area of the ship, and V is hull speed. In the Savitsky method, an equation is obtained to determine the total resistance using Equation 9, as follow [33]:

$$D = \Delta \tan \tau + \frac{D_f}{\cos \tau} \quad (9)$$

where D is the total drag (kN); τ is the trim angle (deg); D_f is the friction component; Δ is the load on the planing surface (craft weight), (N).

Seakeeping analysis

It is critical to accurately estimate ship motion in a complicated maritime environment during the ship design process [34,35]. In obtaining treatment from waves, the ship experienced several movements, including RAO of heaving, rolling, and MSI Index. Heaving is the ship motion that is parallel to the Z-axis, and when heaving occurs, the ship experiences vertical ups and downs caused by waves [35]. Heaving motion is calculated using the formula given in Equation 10 [36]:

$$a\ddot{z} + b\dot{z} + cz = F_0 \cos \omega_e t \quad (10)$$

where a is actual mass, b is damper constant, c is restoring constant, F_0 is amplitude from encountering force, ω_e is encounter frequency, t is time, $\ddot{z}$,$\dot{z}$,z are acceleration, velocity, and displacement, respectively. Rolling is the ship's movement around the longitudinal axis or X-axis. When rolling occurs, the right side of the ship moves to the left side of the ship, which is repeated alternately [35]. This movement should receive attention because it can cause a large dynamic angle, where the wave force will cause extreme rolling excitation. The rolling motion is calculated using the following Equation 11 [36]:

$$a\frac{d^2\Phi}{dt^2} + b\frac{d\Phi}{dt} + c\Phi = M_0 \cos \omega_e t \quad (11)$$

where a is the actual mass of the moment of inertia for rolling, b is coefficient of damping moment, c is coefficient of restoring moment, Φ is phi and $M_0 \cos \omega_e t$ is the outside moment. The work starts with analyzing the motion response at regular waves presented in the Response Amplitude Operator (RAO). RAO is a transfer function that converts the wave force into a dynamic reaction to the structure in the frequency range. The frequency parameter is shown in the abscissa of the RAO graph, and the ratio of the amplitudes of the motion of a certain mode is shown in the ordinate. RAO is a direct comparison between the amplitude of the ship's motion (Za) and the wave's amplitude (ζa), both in length units, for translational motion, as expressed in Equation 12. Meanwhile, RAO for rotational motion is defined as the ratio of the amplitude of the ship's rotation motion (θa) (in radians) to the slope of the wave, see Equation 13.

$$RAO = \frac{Za\ (m)}{\zeta a\ (m)} \quad (12)$$

$$RAO = \frac{\theta a\ (rad)}{k\zeta a\ (rad)} \quad (13)$$

Where ζ = damping ratio, k = wave numbers. Motion sickness incidence (MSI) is a symptom of pain caused by ship movement, which causes uncomfortable physical symptoms characterized by difficulty breathing, dizziness, nausea, paleness, and vomiting [37]. The MSI index is generally used to assess the likelihood of seasickness among crew or passengers. The following is the calculation of the MSI index in Equation 14 [38]:

$$MSI = 100 \left[0.5 \pm erf \left(\frac{\pm \log_{10} \frac{a_v}{g} \pm \mu_{MSI}}{0.4} \right) \right] \quad (14)$$

Where erf is the error function, av is the average vertical acceleration at a specified point or location, The use of the ± sign in the above formula is to indicate that the calculation has two values, namely the + value and – value, and μ_{MSI} is parameters calculated in Equation 15.

$$\mu_{MSI} = -0.819 + 2.32(\log_{10} \omega_E)^2 \quad (15)$$

Where ω_E is encounter frequency

SIMULATION TEST METHOD

This work aims to develop an optimized V-shaped monohull form then perform a comparative analysis to compare the performance of hull shape in terms of stability, resistance, and ship motion to obtain the best hull

shape configuration. The models are designed for race competition with strict design requirements. In this work, the performance of the hull shape is investigated using a numerical method, and then the comparative study is expanded to discuss the calculation process and the results of each method. The models are divided into four main dimensions where the displacement value is used as a fixed parameter. The comparison of particular ship data for model variations can be seen in Table 1.

Table 1: Comparison of particular ship dimensions

Parameter	Model I	Model II	Model III	Model IV
Length overall (m)	0.750	0.700	0.58	0.691
Length Waterline(m)	0.642	0.625	0.558	0.639
Draft (m)	0.053	0.054	0.059	0.049
Beam (m)	0.182	0.182	0.138	0.155
Depth (m)	0.100	0.096	0.086	0.095
Block coefficient	0.301	0.302	0.408	0.383
Displacement (kg)	1.90	1.90	1.90	1.90

In the modification of hull form design, there are several proposed variations, including particular main dimension, changes in the deep V hull shape using variation of deadrise angle, the shape of the bow and transom stern, and the addition effect of fins. The comparison of 3D visualization of four modification models is depicted in Figure 3. Model I has a highest deadrise angle (55o). Model II and Model III has deadrise angle 45o and 40o, respectively. Model IV has same deadrise angle with Model III with adding of fins. The simulation analysis results are represented as graph visualization of each simulation. The result of the stability simulation shows a graph to analyze the relationship between righting arm (GZ) and heel angles. In the stability simulation, the ship is simulated with a heel (the tilt of the ship caused by the influence of external forces) with the heel angle range between 0° and 180° using large-angle stability. The analysis is started by room definition, permeability, and specific gravity. The load case scenario is set to full load condition by defining the lightship and deadweight components. Moreover, the seakeeping test compares heave motion, roll motion, and motion sickness incidence (MSI) graphs between different hull forms. The seakeeping simulation aims to determine the effect of sea conditions on ship motion to achieve the best-proposed hull form. In this case, the height of the wave encounter is assumed at 10 cm at three different levels of Fr, such as 0.5 – 1.0. The angle of encounter wave on the seakeeping test is analyzed in three different conditions, namely beam sea (90°), bow quartering (135°), and head sea (180°). The seakeeping test is conducted using a regular wave aspect with data presented in Table 2. This adjusts to the conditions of the lake waters, where the waves tend to be calm.

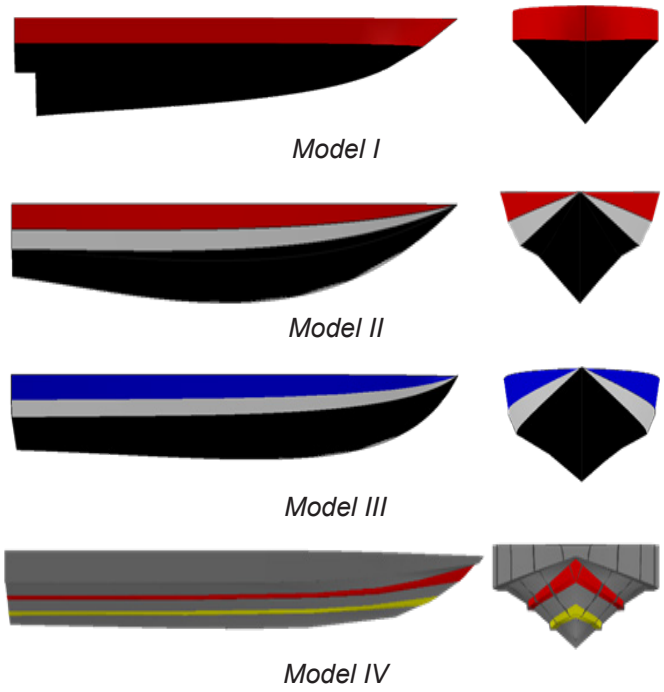

Figure 3: Comparison of 3D hull design of ship models

In the stability simulation, the ship is simulated with a heel (the tilt of the ship caused by the influence of external forces) with the heel angle range between 0° and 180° using large-angle stability. The analysis is started by room definition, permeability, and specific gravity. The load case scenario is set to full load condition by defining the lightship and deadweight components. Moreover, the seakeeping test compares heave motion, roll motion, and motion sickness incidence (MSI) graphs between different hull forms. The seakeeping simulation aims to determine the effect of sea conditions on ship motion to achieve the best-proposed hull form. In this case, the height of the wave encounter is assumed at 10 cm at three different levels of Fr, such as 0.5 – 1.0. The angle of encounter wave on the seakeeping test is analyzed in three different conditions, namely beam sea (90°), bow quartering (135°), and head sea (180°). The seakeeping test is conducted using a regular wave aspect with data presented in Table 2. This adjusts to the conditions of the lake waters, where the waves tend to be calm.

Table 2: Wave spectrum

Type	JONSWAP
Characteristic height	0.100 m
Modal period	9.967 s
Average period	8.346 s
Zero crossing period	7.854 s
Characteristic wind speed	0 knot

Moreover, the resistance test results are presented as a relationship between resistance and power at various ship velocities. This work conducts the analysis using the Savitsky method with a Fr range of 0.5 - 1.0 and 70% power efficiency.

RESULTS AND DISCUSSION

Stability result

This section analyzes the stability test result for all proposed hull form variation models by comparing the relationship between righting arm (GZ) and heel angle, as shown in Figure 4. This figure is plotted assuming that the ship is in static condition. The maximum righting arm (GZmax) and the angle at which it occurs are essential values. In Model I, it can be found that the GZmax is 5.36 cm at 41˚. The GZmax result is proportional to the largest static heeling moment required to bring the ship back to its upright position. In addition, the maximum righting lever, when multiplied with the displacement, represents the value of the maximum heeling moment that the ship can sustain without capsizing. In Model II, GZmax can be found with the value of 2.74 cm at 38.2˚. Moreover, Model III has GZmax value of 0.98 cm at 34.5˚, and Model IV has a maximum GZ at 44.5˚ with a value of 3.05 cm, respectively. After the models experience maximum righting arm, the stability will decrease dramatically as a decrease in the value of righting arm until the points meet the horizontal axis. The results show that the smallest GZmax is experienced by Model III, while the largest GZmax value can be found in Model I. Several factors need to be concerned besides the value of GZmax. Since the GZ value becomes zero where the GZ curve meets the horizontal axis, this condition is assumed at the point of vanishing stability. Any heel angle beyond this will result in unstable equilibrium. Any heel lesser than this angle will allow the vessel to the right itself, while any heel greater than this angle will cause a negative righting moment (or heeling moment) and force the vessel to continue to roll over. When a vessel reaches a heel equal to its point of vanishing stability, any external force will cause the vessel to capsize. The angle range between the initial position and the point of vanishing stability is called the range of stability. According to the data in Figure 4, it can be found that Model I and Model IV have the highest range of stability (above 90˚) compared to other models. The model I and IV will be able to heel to a larger angle before attaining negative stability. In contrast, Model III has the lowest stability range, resulting in a smaller angle before attaining negative stability. As the angle of the heel increases, there comes the point when the deck of the ship immerses, called the angle of deck immersion. It is where the curve changes its gradient and represents the angle of deck edge immersion. When the ship's deck immerses, the rate of shift of the center of buoyancy with further heeling changes, and the main deck will first encounter the sea. This results in a change in the concavity of the curve. The total area under the static stability curve represents the amount of energy that the ship can absorb from external forces such as winds, waves, weight shifts, etc., until it capsizes. As a result, it should not be assumed that a ship is stable enough if the GZmax is high. GZ curve with a very high maximum value may not have enough area, causing the ship to capsize easily because it will not absorb enough energy before capsizing. From the data given in Figure 4, it can be concluded that Model I has the highest energy absorption with the highest maximum righting arm.

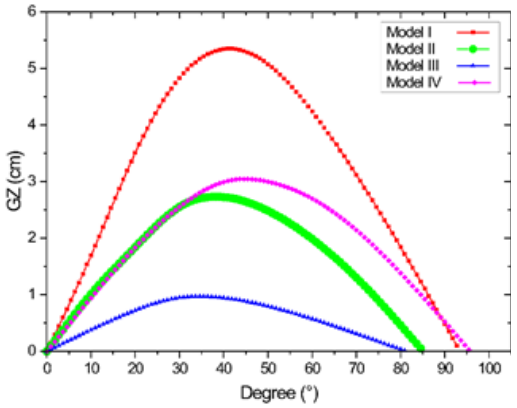

Figure 4: Comparison of GZ curve at different heel angles

Result of resistance and powering

Further, the comparison of the resistance test will be discussed in this section. The comparison test result of the resistance and powering of all proposed 3D models are depicted in Figure 5a and 5b, respectively. The resistance test is calculated from the Froude number (Fr) range between 0.5 and 1 using Savitsky analytical method. The Froude number is a dimensionless speed, where the velocity in metres per second is divided by the square root of the length of waterline (LWL) times the acceleration of gravity. Validation test between analytical method using Eq. 9 and numerical simulation using Maxsurf resistance depicted in Table 3 shows a good agreement with the error below 5%. From the resistance result shown in Figure 5a, it can be found that the higher the Froude number, the higher the resistance of all developed models. Therefore, it can be found that Model III experiences the highest resistance compared with other hull form types. In contrast, the smallest resistance can be found in Model II in small Fr, but in high Fr, the smallest resistance can be found in Model I. It can be realized that Model III has the biggest block coefficient (Cb) value compared with three other designs. It can be found that the higher the block coefficient (Cb) of the ship, the wetted surface area will increase. In a detailed explanation, the comparative result of the resistance and power at a Fr 1.0 shows that Model I has a resistance of 3.34 N and the required power of 11.97 W. Model I has a resistance value of 19.1% lower than Model III. Moreover, Model IV has a higher resistance compared with Model I, with a value of 3.5 N and the required power of 12.54 W. Then, Model II has a resistance of 3.51 N and the required power of 12.43 W at Fr 1. Model III has the highest resistance and power value of about 4.13 N and the power of 13.79 W, respectively.

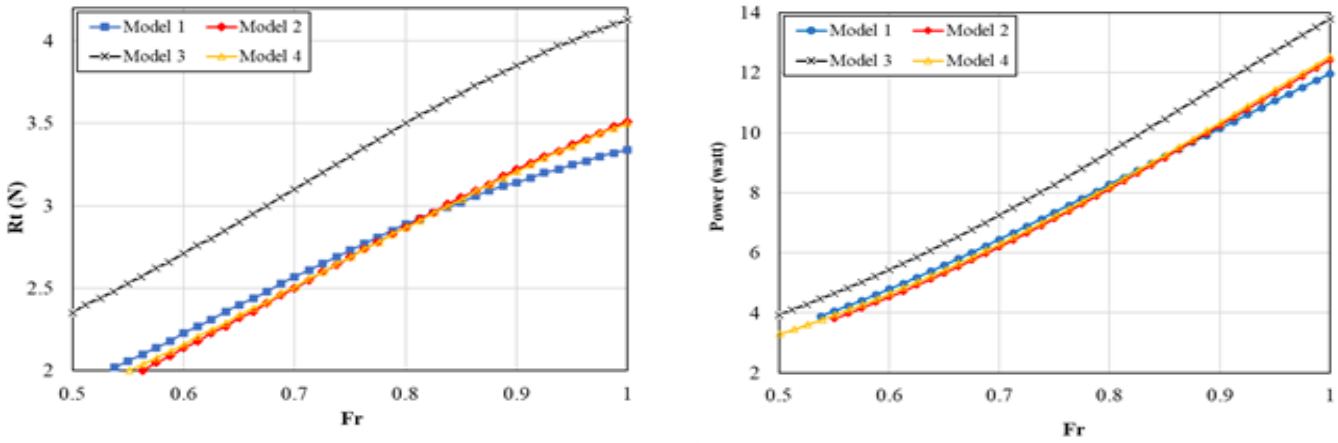

(a) (b)

Figure 5: Comparative result of (a) resistance with speed; (b) power with speed

Table 3: Resistance validation test

Model	Resistance at Fr 1.0 (N)		Error (%)
	Analytical method	Numerical simulation (Maxsurf)	
Model I	3.26	3.34	2.45
Model II	3.42	3.51	2.63
Model III	4.01	4.13	2.99
Model IV	3.41	3.50	2.64

Ship motion result

A ship above sea level will always get an external force that causes the ship's motion. External factors, especially waves, cause this ship's motion. Therefore, seakeeping analysis aims to investigate the comparative heaving and rolling motion and passenger comfort between all proposed models analyzed at various Fr ranging from low Fr to high Fr. The discussion is divided into the result of ship motion response at Fr 0.5 – 1.0 with three different wave directions.

Ship motion response at Fr 0.50

Seakeeping test results of the hull form variations, including heave motion, roll motion, and MSI, are discussed at similar Fr 0.50. The relation between heave RAO and encounter frequency at Fr 0.5 analyzed in three different wave directions is plotted in Figure 6. From the result, it can be found that Model III has the highest heave RAO value in all three different wave headings. In contrast, Model I has the lowest heave RAO amplitude. Analyzing motion response due to wave heading from the side of the ship as presented in Figure 6a, it can be found that heave motion due to beam sea does not have a significant response, represented by lower RAO peak magnitude compared to the heave motion due to bow quartering sea (Figure 6b) and head sea (Figure 6c). However, the heave motion due to beam sea experiences a superposition due to the occurrence of more than two peaks of wave frequency, which will cause the ship to move irregularly. Moreover, the highest heave RAO response can be found in the head sea wave heading and followed by bow quartering sea. It means that wave heading from the head sea (180 degrees) causes the increase of heave RAO response more significantly than other wave heading of the proposed hull form models. It can also be analyzed that there is no superposition found in the heave RAO response from bow quartering sea and head sea conditions. The ship does not receive more than one wave, and this condition is more stable if there is a wave from that direction. Compared to the heave RAO response between different hull forms, it can be concluded that Model I is the best model in heave motion to encounter the wave force from three different wave headings at Fr 0.5. Besides heave RAO response, the comparison result of roll RAO at different wave headings is also a crucial point. Figure 7 shows the comparison result of varied hull form designs of roll RAO at different wave headings. The roll RAO with the wave heading from the 90˚ (beam sea) and the 135˚ direction (bow quartering) has almost the same peak of roll RAO and encounter frequency of all hull form models, except Model III, which has a lower peak of wave frequency. Moreover, Model IV has a slightly smaller peak roll RAO, which means it is slightly more stable so that the rolling motion or right-handed motion is smaller relative to the incoming wave. In contrast, the arrival of waves from the direction of 180˚ (head sea) has a rolling value of 0 because the arrival of waves from the front does not affect the ship's left and right rolling motion. From the comparison results of the RAO rolling graph with the RAO wave frequency graph, there is no superposition at the top of the graph. So that the ship does not receive more than one wave, this condition of the ship is more stable if there are waves from that direction.

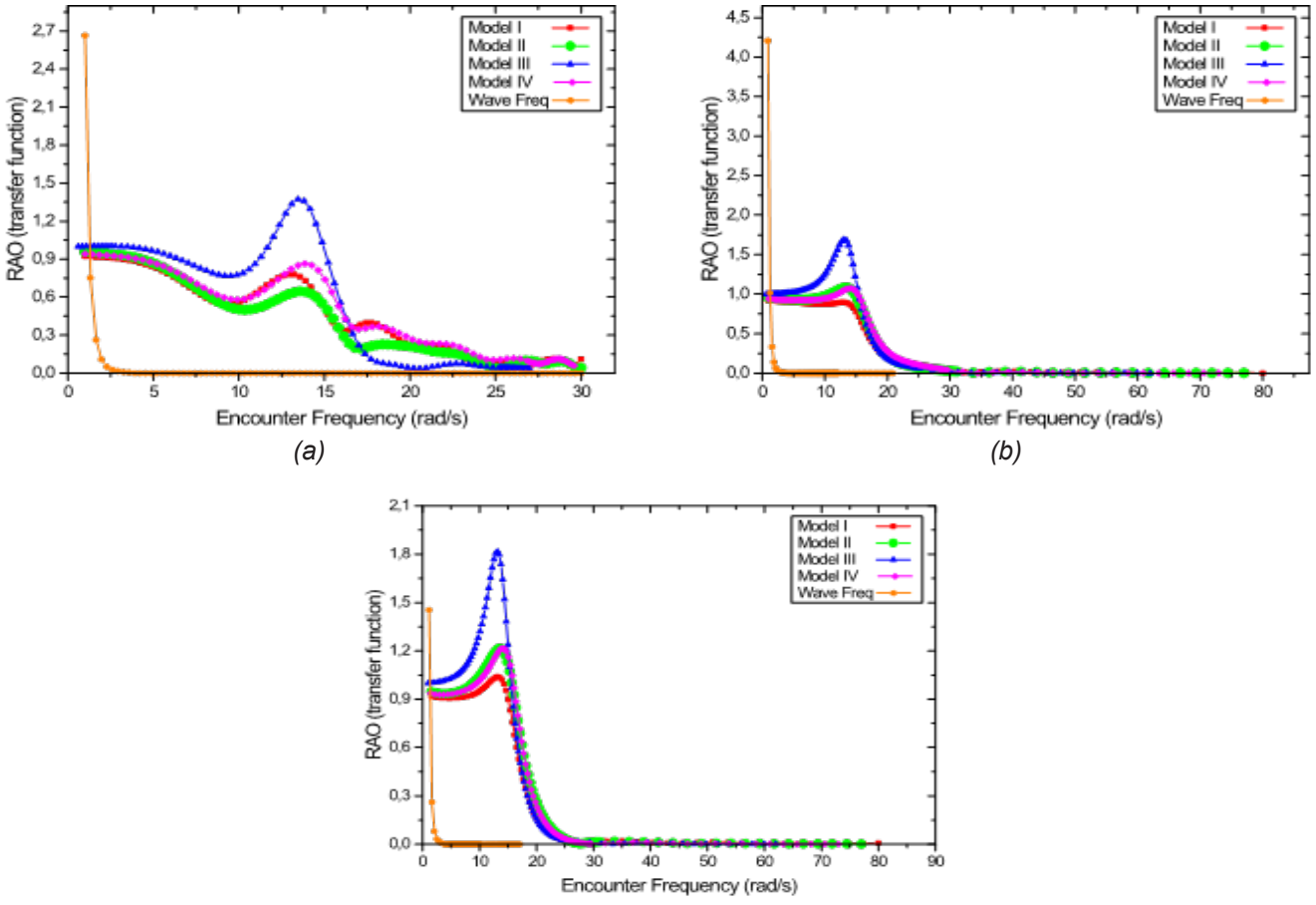

Figure 6: Heave RAO at Fr 0.5 with the angle of coming waves (a) 90°; (b) 135°; (c) 180°

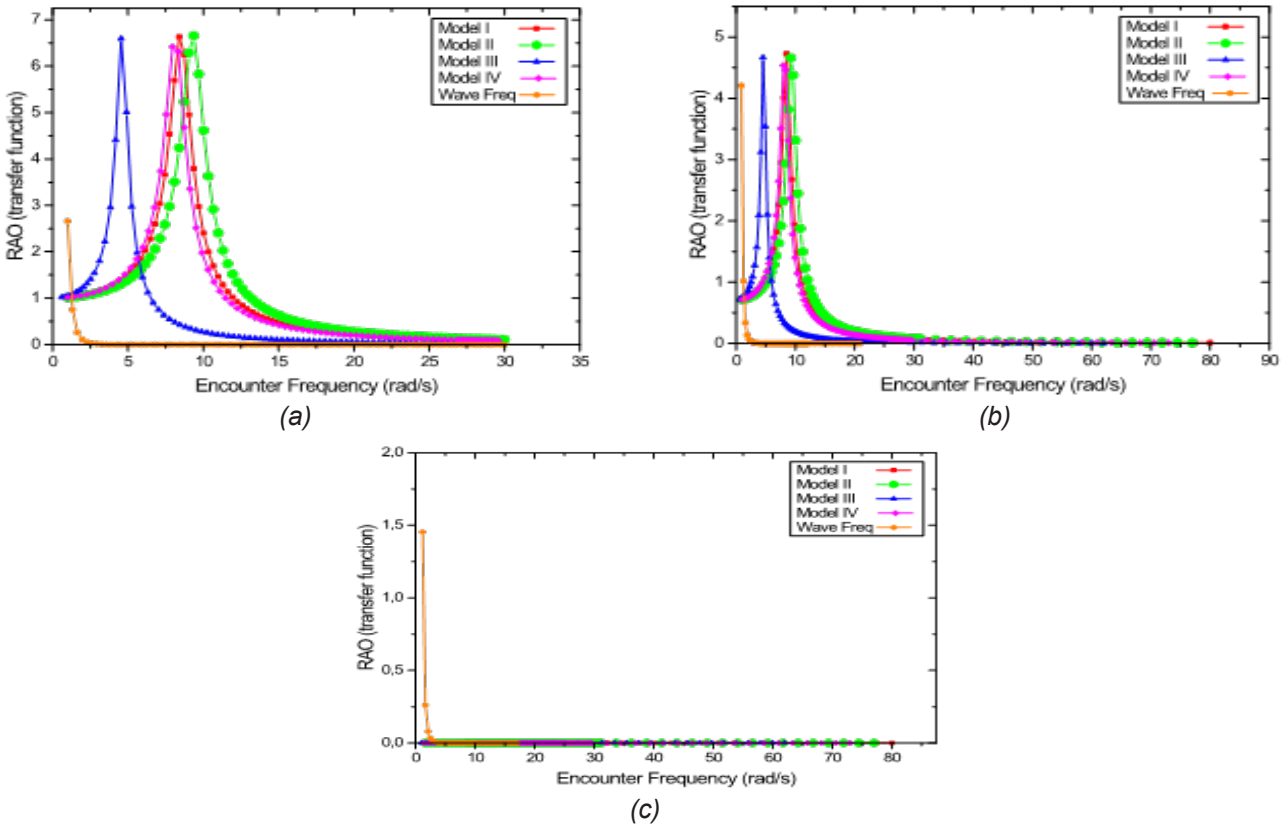

Figure 7: Roll RAO at Fr 0.5 with heading angle of the ship against wave (a) 90°; (b) 135°; (c) 180°

Motion Sickness Incidence (MSI), chosen as a parameter to estimate the seakeeping qualities of a high-speed, is defined as the mean MSI over the main deck area for any different heading angle. MSI was also embodied in 1985, where severe discomfort boundary values of ship vertical accelerations are defined as motion exposure time and encounter frequency. The role of accelerations for the occurrence of MSI is appreciable onboard high-speed vessels (Fn>0.50). MSI is defined as the percentage of passengers who vomit after 2 hours of exposure to a specific motion. R.M.S. of vertical acceleration at remote control points at ship deck is defined as a function of the encounter frequency. Model I, II, III, and IV have stable levels or do not cause shocks that cause MSI to meet the requirements. There are no vertical acceleration values from each model that cut the graph of the percentage of MSI provisions after 2 hours. As seen in the encounter frequency 0 – 10 rad/s, there is an increase in the acceleration value for each model, but it does not cut the MSI graph. So there is no seasick passenger with a model design made at Fr 0.50 with waves from 90˚, 135˚, and 180˚.

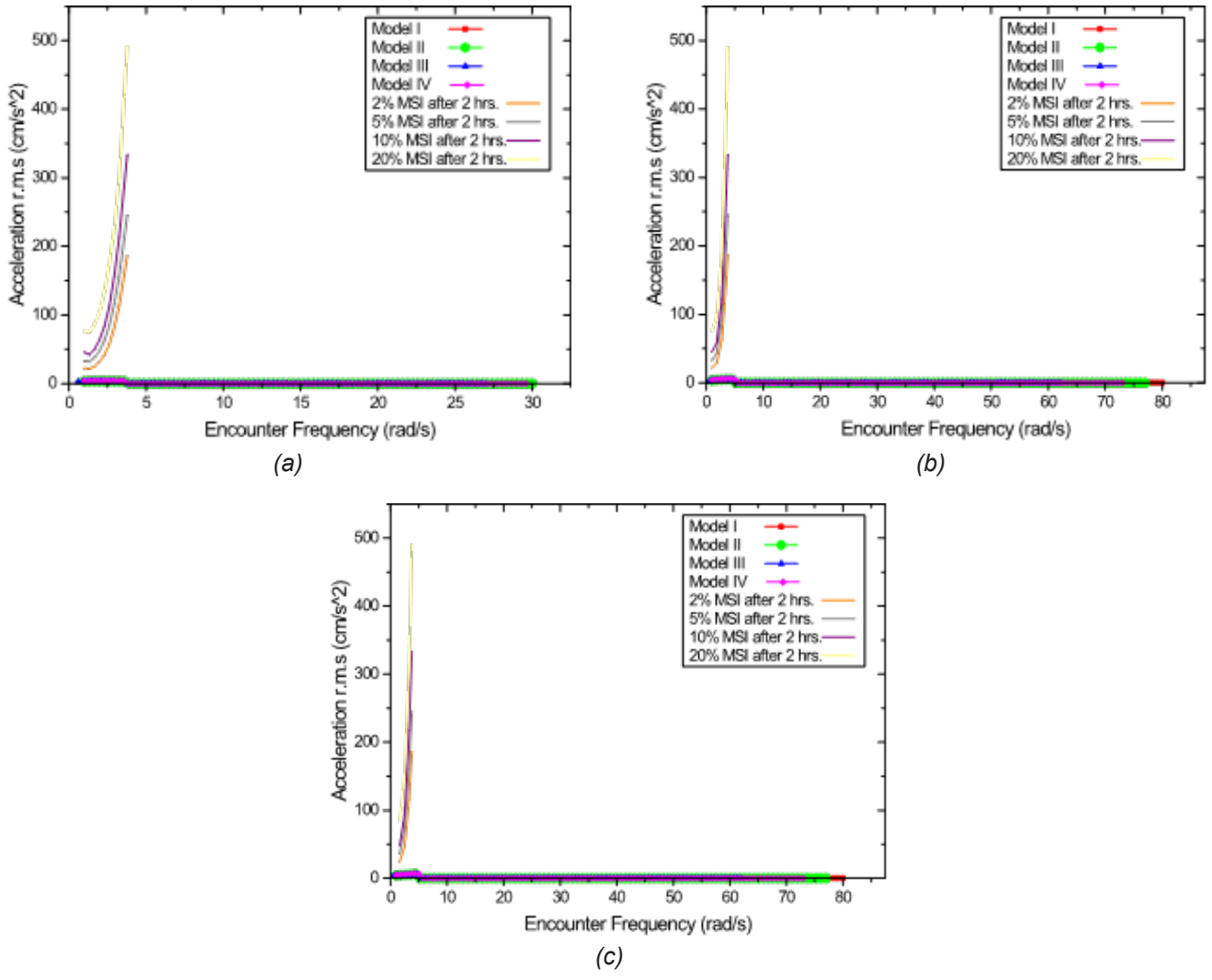

Figure 8: Graphic MSI at Fr 0.5 with heading angle of the ship against wave (a) 90°; (b) 135°; (c) 180°

Ship motion response at Fr 0.75

It is important to analyze the ship's motion behavior at high speed. Comparison of RAO heave, roll RAO, and MSI at a Fr 0.75 is depicted in Figures 9-11. The comparison of heave RAO analyzed at three different wave headings shown in Figure 9 results in a similar phenomenon with heave motion at previous Fr. It can be analyzed that the heave RAO at Fr 0.75 has a higher response than the heave response at Fr 0.5. It can be found that Model III has the highest peak of heave RAO in all wave headings. In contrast, Model I has better seakeeping behavior due to having the lowest peak of heave RAO response. Further, it can be found that heave motion due to beam sea (90 degrees) in Figure 9a does not have a significant response, represented by lower RAO peak magnitude compared to the heave motion due to bow quartering sea (Figure 9b) and head sea (Figure 9c). The heave motion caused by beam sea, on the other hand, undergoes a superposition due to two peaks of wave frequency, causing the ship to move unevenly.

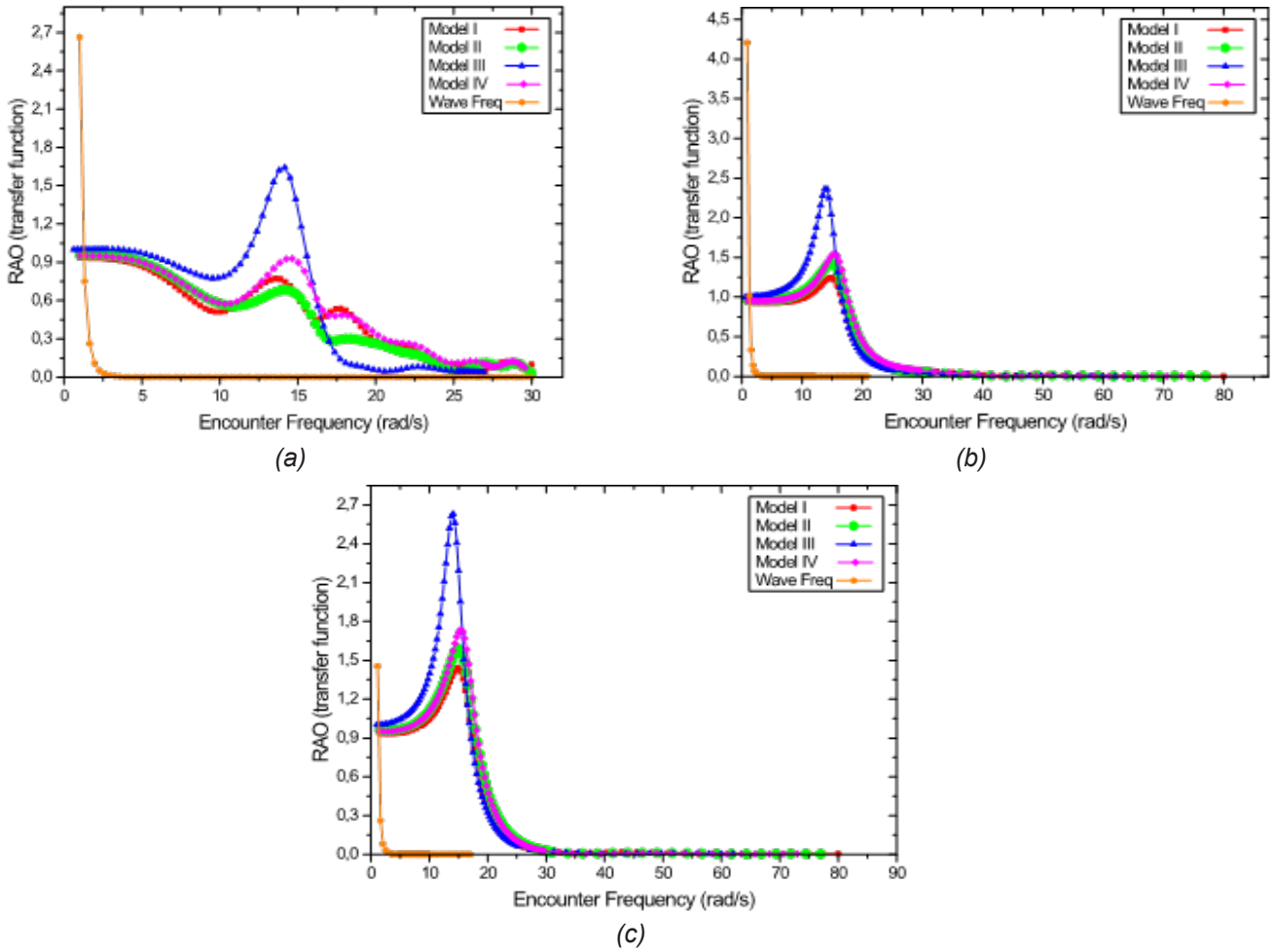

Figure 9: Heave RAO at Fr 0.75 with heading angle of the ship against wave (a) 90°; (b) 135°; (c) 180°

Furthermore, the most significant heave RAO response is seen in the head sea wave heading, followed by the bow quartering sea. The wave heading from the head sea (180 degrees) generates a more significant rise in heave RAO motion than other wave headings of the proposed hull form models. It is also possible to see that there is no superposition in the heave RAO response between bow quartering sea and head sea scenarios. The ship receives only one wave, and this state is steadier if there is a wave from that direction. Figure 10 depicts a comparison of roll RAO results at various wave headings. The maximum roll RAO can be seen in the models at beam sea, which is a similar phenomenon to the prior finding at Fr 0.5. The roll RAO of the models at beam seas is slightly higher than the response of bow quartering seas. At beam and bow quartering seas, all models almost have the same peak RAO in various encounter frequencies. In addition, Model III has a heave RAO peak in lower encounter frequency than other hull models. The arrival of waves from the front, on the other hand, has a rolling value of 0 since the arrival of waves from the front has no effect on the ship's rolling motion. There is no superposition based on the comparison findings of the roll RAO and encounter frequency. This situation of the ship is steadier if there are waves from that direction so that the ship does not get more than one wave. In addition to the ship's motion, the MSI criteria are required to compare the passenger comfort index. The MSI value of Models I, II, III, and IV is determined to be stable or does not produce shocks. It may be discovered that ship motion at a Fr 0.75 satisfies the requirements since there is no graph from each model that cuts the graph of the MSI % after 2 hours. As observed in the encounter frequency 0 – 10 rad/s, there is a rise in acceleration value for each model. However, it does not cut the MSI graph. As a result, none of the offered models had a seasick passenger at Fr 0.75 with waves in three distinct wave direction situations.

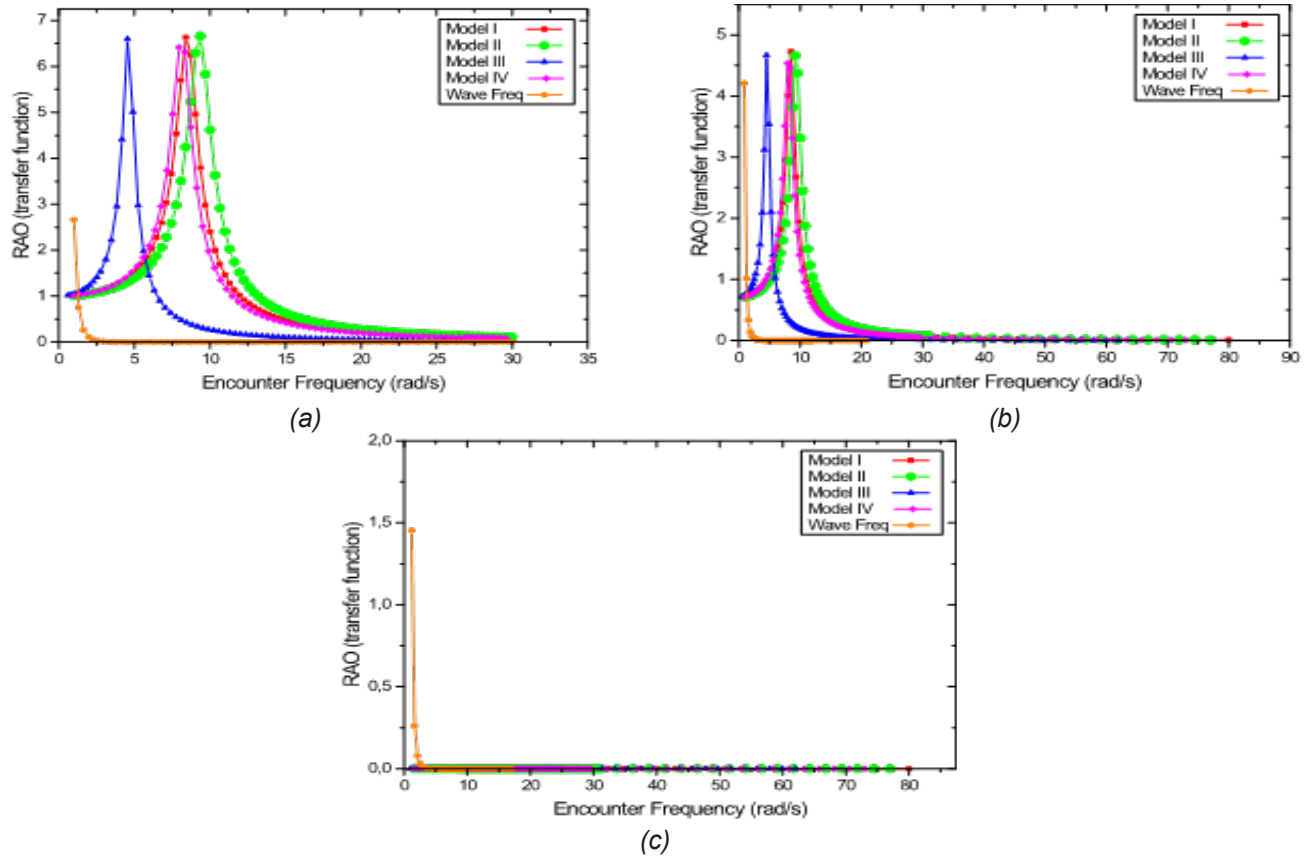

Figure 10: Roll RAO at Fr 0.75 with the heading angle of the ship against wave (a) 90°; (b) 135°; (c) 180°

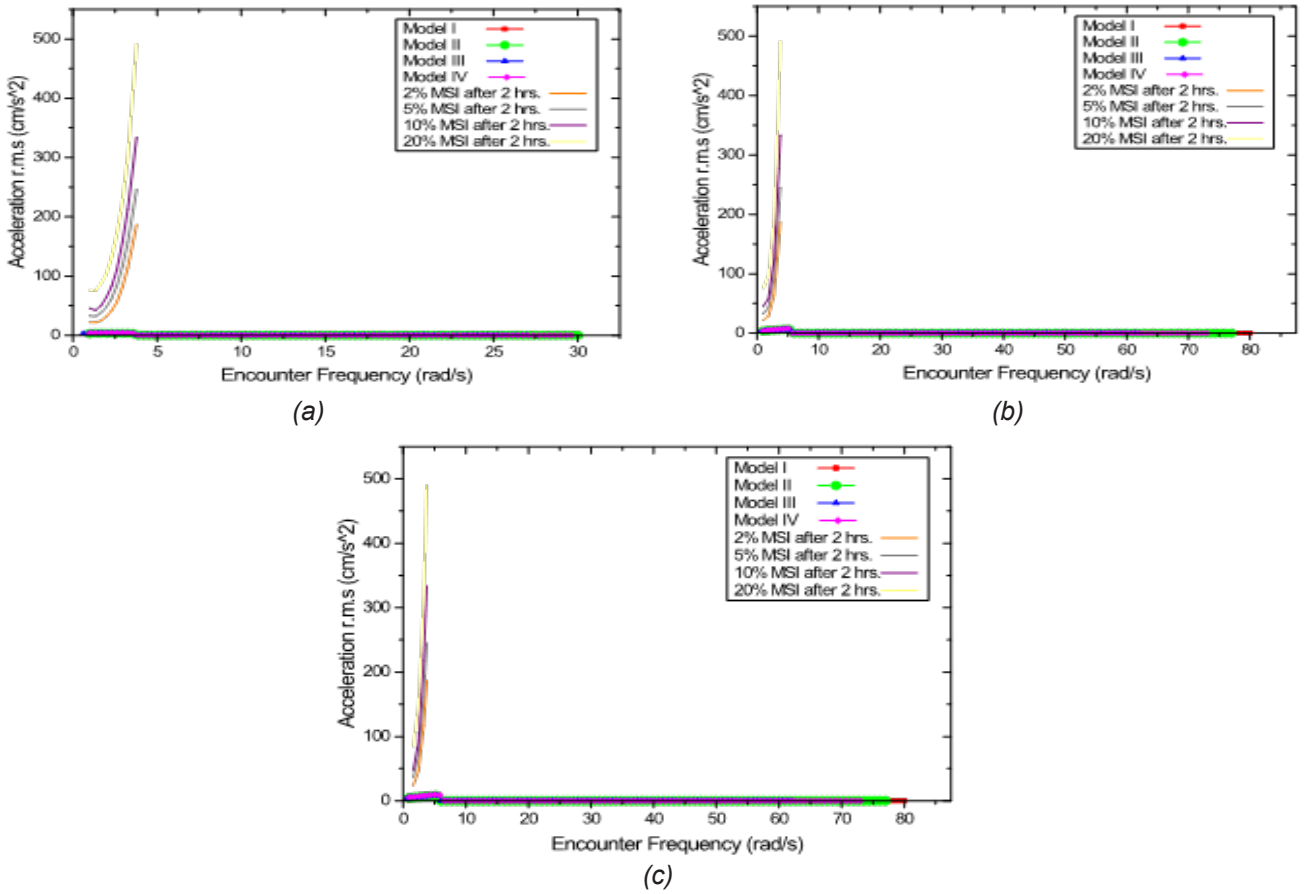

Figure 11. Graphic MSI at Fr 0.75 with the heading angle of the ship against wave (a) 90°; (b) 135°; (c) 180°.

Ship motion response at Fr 1.0

At last, the investigation of ship motion response at Fr 1,0 is discussed. The comparison result of heave RAO, roll RAO, and MSI at Fr 1.0 is depicted in Figures 12-14. Figure 12 illustrates the comparison of heave RAO analyzed at three different wave headings, resulting in a similar phenomenon with heave motion at two previous Fr. It can be analyzed that the heave RAO at Fr 1.0 has a higher response than the heave response at previous lower Fr. It can be found that the heave RAO at beam seas does not have a significant effect on the ship motion compared with the ship at load wave at bow quartering and head seas, representing by the lowest peak of heave motion. It is found that Model I has better seakeeping behavior in all wave headings represented by the lowest peak heave RAO response compared to other models. In the heave response due to beam sea (90 degree) in Figure 12a, it can be chosen that Model III has the almost highest twice of heave RAO peaks, but Model I and II have the lowest value with almost the same peak value. Similar to the previous case, heave motion caused by beam sea undergoes a superposition due to two peaks of wave frequency, causing the ship to move unevenly. Moreover, the most significant heave RAO response is seen in the head sea wave heading, followed by the bow quartering sea. Both Model III has the highest peak of heave motion, and the lowest one can be found in Model I. There is also no superposition in the heave RAO motion for bow quartering sea and head sea situations. The ship only gets one wave, and this state is more stable if a wave comes from that direction.

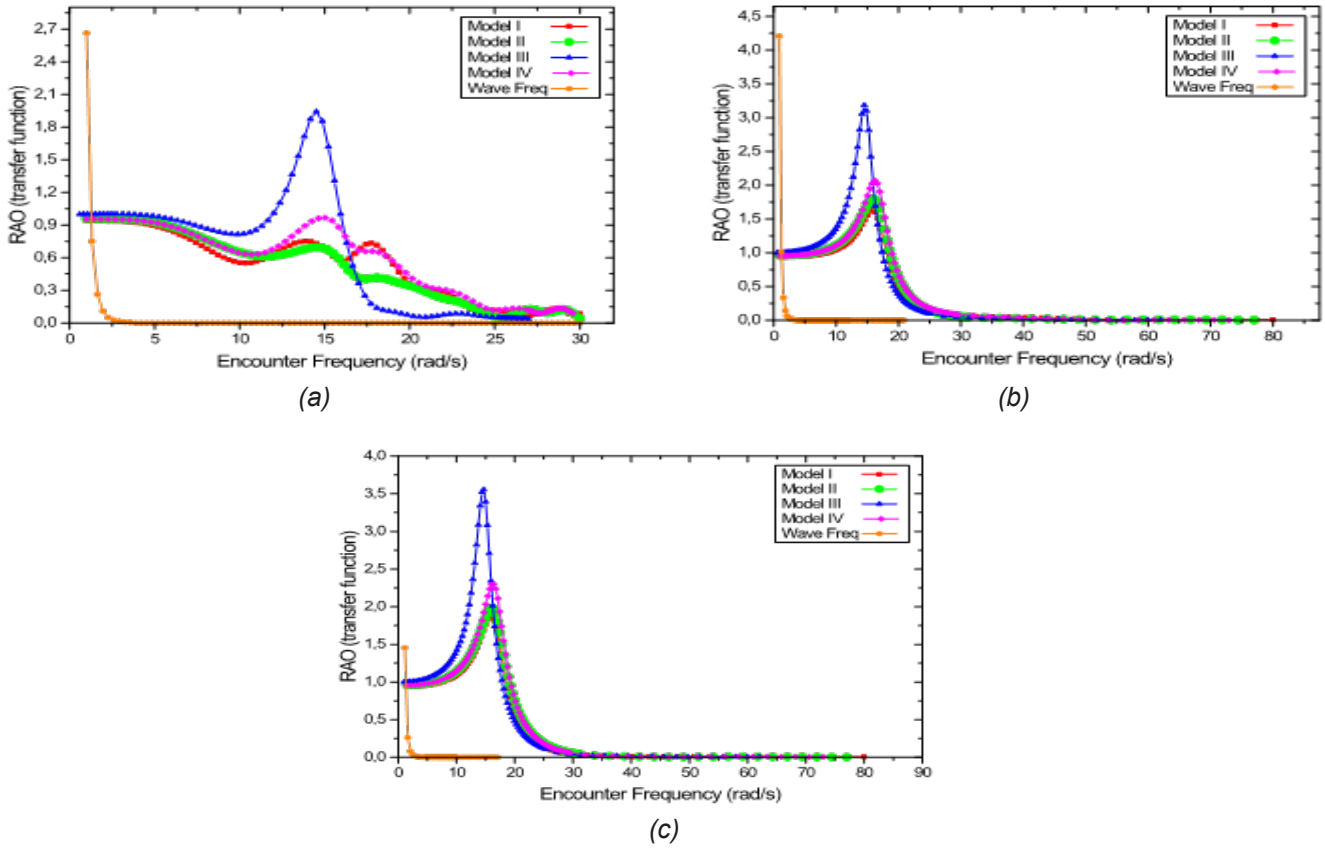

Figure 12: Heave RAO at Fr 1.0 with the heading angle of the ship against wave (a) 90°; (b) 135°; (c) 180°

The comparison of roll RAO results at Fr 1.0 with various wave headings can be found in Figure 13. The maximum roll RAO can be seen in the models at beam sea and followed by bow quartering sea, which is similar to the previous case. In contrast, there is no roll motion if the ship encounters a wave from the head sea, as seen in Figure 13c. The roll RAO of the models at beam seas and bow quartering seas has a nearly identical peak of heave motion on all hull form models. It is found that there is no superposition of the roll RAO and encounter frequency in all evaluated wave headings. In addition, the MSI criteria are also discussed to compare the passenger comfort index analyzed at high speed. The MSI value of all evaluated models due to high speed is determined to be stable or does not produce shocks, as shown in Figure 14. It may be discovered that ship motion at Fr 1.0 satisfies the comfort requirements. As observed in the encounter frequency 0 – 10 rad/s, each model has a rise in acceleration value; however, it does not cut the MSI graph.

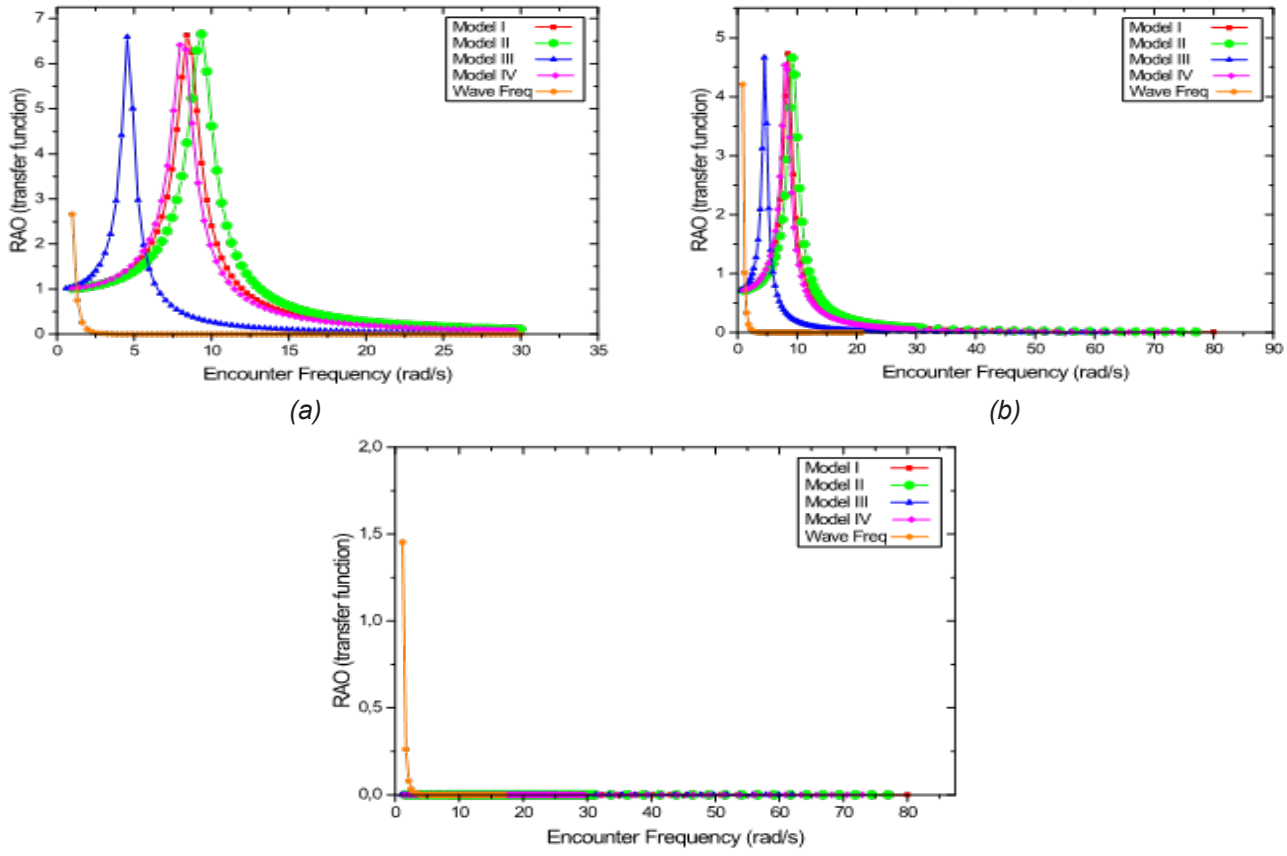

Figure 13: Roll RAO at Fr 1.0 with the heading angle of the ship against wave (a) 90°; (b) 135°; (c) 180°

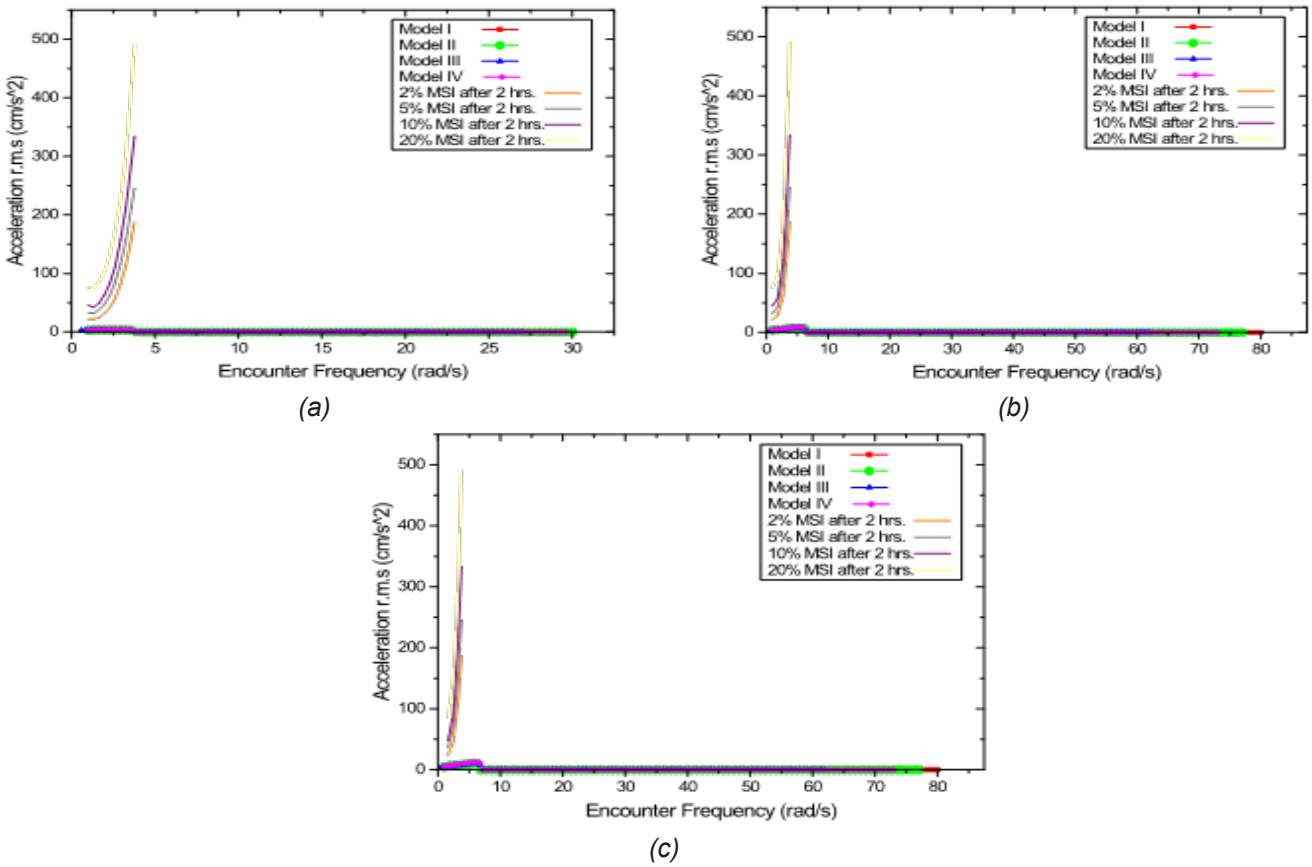

Figure 14: MSI at Fr 1.0 with the heading angle of the ship against wave (a) 90°; (b) 135°; (c) 180°

Overall discussion

The ship model has been tested and analyzed on each model in accordance with predetermined criteria, namely stability, resistance, and seakeeping. Then the data is compared to determine the best design can be seen in Table 4 based on the designer's criteria in Table 5. Based on Table 5, there are three general criteria and one specific criterion. The first criterion regarding stability, the value of the total area under the static stability curve, represents the amount of energy that can be absorbed by the ship from external forces such as wind, waves, weight shift, etc. until the ship capsized. Ships that do not have a sufficient area under the curve cause the ship to easily capsize because it does not absorb enough energy before capsizing. Therefore, it takes a ship with a stability value of the area under the greatest curve. The second criterion is resistance, the resistance of the fluid passing through the ship and it affects the performance of the ship. Ships that have a small resistance value will be more optimal when sailing, so this research requires an optimal ship and has the smallest resistance value. The third criterion is seakeeping here, and there are heaving and rolling tests. Heaving is the up and down motion of the ship and the rolling motion of the ship's right and left caused by waves. If a ship has a large heaving and rolling value, the shaking (up and down motion and left and right motion) of the ship will get bigger and become unstable. In this case, preferred seakeeping is needed for the ship to remain stable, namely by having the smallest seakeeping value so that it can minimize shocks. This particular criterion is the most important thing in the competition that we want to enter requires the best time with limited supply. The specific criteria are the resistance test because the limited use of batteries in competition requires a small resistance value to reach the maximum and optimal time. Based on Table 4, the value is the best in each criterion marked in bold. Based on data in Table 5, the general criteria, stability, which has a large value, is preferred, while resistance and seakeeping, which has a small value, is preferred. In this special criteria, the most important aspect is the resistance test due to the limited use of batteries in race competition, so a small resistance value is needed for optimal results. It is found in Table 4 that Model I is superior in terms of stability, seakeeping, and resistance performances. As a result, Model I is chosen as the best hull model.

CONCLUSIONS

From the comparative results of the performance of high-speed craft in various hull forms in terms of stability, resistance, and seakeeping tests, it can be concluded that:

1. It can be found that Model I has satisfactory initial stability, which is the highest righting arm, and energy absorption due to the external force.
2. From the data obtained, the faster the ship's velocity, the more resistance will increase. It is concluded that Model I has less resistance and power than the other designs. However, the highest value can be found in Model III. The ship is more ideal when sailing on the sea with less resistance, and the engine was supposed to be more optimal with less power required.
3. In the seakeeping test, which was analyzed at different Fr and three different wave directions, it can be seen that Model I has better behavior of heave motion, but model IV has better performance of roll motion. However, Motion Sickness Incident (MSI) meets the requirements of passenger comfort levels,

Table 4: Data for each model

Criteria		Model			
		Model I	Model II	Model III	Model IV
Stability	Area under GZ curve (cm.deg)	303.2	144.6	47.8	181.7
	Max GZ (cm)	5.36	2.74	0.98	3.05
	Angle of vanishing stability	92.7	83.6	80.0	96.4
Resistance	Resistance (N)	3.34	3.51	4.13	3.5
Seakeeping	Max heaving (rad/s)	1.95	1.98	3.62	2.31
	Max rolling (rad/s)	6.63	6.64	6.61	6.52

Table 5: General and specific criteria

General Criteria			Specific Criteria
Stability	Resistance	Seakeeping	
Large value is preferred	Large value is unprefered	Large value is unprefered	The resistance & power aspect is prioritized
Small value is unprefered	Small value is preferred	Small value is preferred	

which are analyzed at three different Fr and wave directions. It was found that none of the results from any model intersects the MSI percentage chart after 2 hours. The result of the designed model, no seasick passengers.

4. 4. The best ship is based on specific criteria. Namely, the important aspect is resistance, so for the best design, Model I is selected with the lowest resistance value and best seakeeping and stability performances.
5. 5. Extended investigation is recommended to be conducted, especially in terms of minimizing resistance by considering the maximum gravity-to-metacenter point. To achieve wider hull performance data, propulsion analysis, e.g., cavitation, may be selected as one of the potential topics.

REFERENCES

1. Costanza, R. (1999). The ecological, economic, and social importance of the oceans. Ecological economics, vol. 31, no. 2, 199-213, DOI: 10.1016/S0921-8009(99)00079-8
2. Prabowo, A.R., Laksono, F.B., Sohn, J.M. (2020). Investigation of structural performance subjected to impact loading using finite element approach: Case of ship-container collision. Curved and Layered Structures, vol. 7, 17–28, DOI: 10.1515/cls-2020-0002
3. Prabowo, A.R., Muttaqie, T., Sohn, J.M., Bae, D.M. (2018). Nonlinear analysis of inter-island roro under impact: Effects of selected collision's parameters on the crashworthy double-side structures. Journal of the Brazilian Society of Mechanical Sciences and Engineering, vol. 40, no. 5, 248, DOI: 10.1007/s40430-018-1169-6
4. Prabowo, A.R., Baek, S.J., Cho, H.J., Byeon, J.H., Bae, D.M., Sohn, J.M. (2017). The effectiveness of thin-walled hull structures against collision impact. Latin American Journal of Solids and Structures, vol 14, no. 7, 1345-1360, DOI: 10.1590/1679-78253895
5. Prabowo, A.R., Bae, D.M., Sohn, J.M. (2019). Comparing structural casualties of the Ro-Ro vessel using straight and oblique collision incidents on the car deck. Journal of Marine Science and Engineering, vol. 7, no. 6, 183, DOI: 10.3390/jmse7060183
6. Prabowo, A.R., Sohn, J.M. (2019). Nonlinear dynamic behaviors of outer shell and upper deck structures subjected to impact loading in maritime environment. Curved and Layered Structures, vol. 6, 146–160, DOI: 10.1515/cls-2019-0012
7. Prabowo, A.R., Muttaqie, T., Sohn, J.M., Harsritanto, B.I.R. (2019). Investigation on structural component behaviours of double bottom arrangement under grounding accidents. Theoretical and Applied Mechanics Letters, 2019, vol. 9, no. 1, 50–59, DOI: 10.1016/j.taml.2019.01.010
8. Prabowo, A.R., Cao, B., Sohn, J.M., Bae, D.M. (2020). Crashworthiness assessment of thin-walled double bottom tanker: Influences of seabed to structural damage and damage-energy formulae for grounding damage calculations. Journal of Ocean Engineering and Science, vol. 5, no. 4, 387–400, DOI: 10.1016/j.joes.2020.03.002
9. Yusvika, M., Prabowo, A.R., Tjahjana, D.D.D.P., Sohn, J.M. (2020). Cavitation prediction of ship propeller based on temperature and fluid properties of water. Journal of Marine Science and Engineering, vol. 8, no. 6, 465, DOI: 10.3390/JMSE8060465
10. Cao, B., Bae, D.-M., Sohn, J.-M., Prabowo, A.R., Chen, T.H., Li, H. (2016). Numerical analysis for damage characteristics caused by ice collision on side structure. The 35th International Conference on Offshore Mechanics and Arctic Engineering (OMAE), Busan, South Korea. Article number: V008T07A019.
11. Genda, H. (2016). Origin of Earth's oceans: An assessment of the total amount, history and supply of water. Geochemical. Journal, vol. 50, no. 1, 27–42, DOI: 10.2343/geochemj.2.0398
12. Prabowo, A.R., Tuswan, T., Ridwan R. (2021). Advanced Development of Sensors' Roles in Maritime-Based Industry and Research: From Field Monitoring to High-Risk Phenomenon Measurement. Applied Sciences, vol. 11, no. 1, 3954, DOI: 10.3390/app11093954
13. Julianto, R.I., Prabowo, A.R., Muhayat, N., Putranto, T., Adiputra, R. (2021). Investigation of Hull Design to Quantify Resistance Criteria using Holtrop's Regression based Method and Savitsky's Mathematical Model: A Study Case of Fishing Vessels. Journal of Engineering Science and Technology, vol. 16, no. 2, 1426 - 1443, DOI: -
14. Febrianto, R.A., Prabowo, A.R., Baek, S.J., Adiputra, R. (2021). Analysis of Monohull Design Characteristics as Supporting Vessel for the COVID-19 Medical Treatment and Logistic. Transportation Research Procedia, vol. 55, 699-706, DOI: 10.1016/j.trpro.2021.07.038
15. Bahatmaka, A., Prabowo, A.R., Kim, D.J. (2021). Effect of Nozzle Performance on the Ducted Propeller: A Benchmark-Simulation Study using OpenFOAM. Transportation Research Procedia, vol. 55, 645-652, DOI: 10.1016/j.trpro.2021.07.031
16. Nugroho, A., Khaeroman, Nubli, H., Prabowo, A.R., Yudo, H. (2020). Finite Element Based Analysis of Steering Construction System of ORCA Class Fisheries Inspection Ship. Procedia Structural Integrity, vol. 27, 46-53, DOI: 10.1016/j.prostr.2020.07.007
17. Prabowo, A.R., Martono, E., Muttaqie, T., Tuswan, T., Bae, D.M. (2022). Effect of hull design variations on the resistance profile and wave pattern: a case study of the patrol boat vessel. Journal of Engineering Science and Technology, vol.17, no. 1, 106–126, DOI: -

18. Julianto, R.I., Muttaqie, T., Adiputra, R., Hadi, S., Hidajat, R.L.L.G., Prabowo, A.R. (2020). Hydrodynamic and Structural Investigations of Catamaran Design. Procedia Structural Integrity, vol. 27, 93-100, DOI: 10.1016/j.prostr.2020.07.013
19. Zhao, Y., Zong, Z., Zou, L. (2015). Ship hull optimization based on wave resistance using wavelet method. Journal of Hydrodynamics, vol. 27, 216-222, DOI: 10.1016/S1001-6058(15)60475-9
20. Chrismianto, D., Tuswan, Manik, P. (2018). Analysis of Resistance and Effective Wake Friction due to Addition of Stern Tunnels on Passenger Ship Using CFD. IOP Conference Series Earth and Environmental Science, vol. 135, 012008, DOI: 10.1088/1755-1315/135/1/012008
21. Yanuar, Ibadurrahman, I., Gunawan, A., Wibowo, R.A., Gunawan. (2020). Drag reduction of X-pentamaran ship model with asymmetric-hull outrigger configurations and hull separation. Energy Report, vol. 6, 784-789, DOI: 10.1016/j.egyr.2019.11.158
22. Esmailian, E., Gholami, H., Røstvik, H.N., Menhaj, M.B. (2019). A novel method for optimal performance of ships by simultaneous optimisation of hull-propulsion-BIPV systems, vol. 197, 111879, DOI: 10.1016/j.enconman.2019.111879
23. Rosén, A., Begovic, E., Razola, M., Garme, K. (2017). High-speed craft dynamics in waves: challenges and opportunities related to the current safety philosophy. The 16th International Ship Stability Workshop (ISSW 2017), Belgrade, Serbia. Article number: -
24. Scamardella, A., Piscopo, V. (2014). Passenger ship seakeeping optimization by the Overall Motion Sickness Incidence. Ocean Engineering, vol. 76, 86-97, DOI: 10.1016/j.oceaneng.2013.12.005
25. Piscopo, V., Scamardella, A. (2015). The overall motion sickness incidence applied to catamarans. International Journal of Naval Architecture and Ocean Engineering, vol. 7, no. 4, 655- 669, DOI: 10.1515/ijnaoe-2015-0046
26. Lopez, E., Velaseo, F.J., Rueda, T.M., Moyano, E. (2003). Experiments on the Reduction of Motion Sickness Incidence on a High-Speed Craft. IFAC Proceedings, vol. 36, no. 21, 97-102, DOI: 10.1016/S1474-6670(17)37790-X
27. Ashkezari, A.Z., Moradi, M. (2021). Three-dimensional simulation and evaluation of the hydrodynamic effects of stern wedges on the performance and stability of high-speed planing monohull craft. Applied Ocean Research, vol. 110, 102585, DOI: 10.1016/j.apor.2021.102585
28. Manderbacka, T., Themelis, N., Bačkalov, I., Boulougouris, E., Eliopoulou, E., Hashimoto, H., Konovessis, D., Leguen, J-F., González, M., Rodríguez, C.A., Rosén, A., Ruponen, P., Shigunov, V., Schreuder, M., Terada, D. (2019). An overview of the current research on stability of ships and ocean vehicles: The STAB2018 perspective. Ocean Engineering, vol. 186, 106090, DOI: 10.1016/j.oceaneng.2019.05.072
29. Im, N. K., Choe, H. (2021). A quantitative methodology for evaluating the ship stability using the index for marine ship intact stability assessment model. International Journal of Naval Architecture and Ocean Engineering, vol. 13, 246–259. DOI: 10.1016/j.ijnaoe.2021.01.005
30. Barrass, B., Derrett, D.R. (2006). Ship Stability For Masters And Mates, Sixth edition. Butterworth-Heinemann, Oxford.
31. Poundra, G.A.P., Utama, I.K.A.P., Hardianto, D., Suwasono, B. (2017). Optimizing trimaran yacht hull configuration based on resistance and seakeeping criteria. Procedia Engineering, vol. 194, 112–119, DOI: 10.1016/j.proeng.2017.08.124
32. Tupper, E.C. (2013). Introduction to Naval Architecture, Fifth edition. Butterworth-Heinemann, Oxford.
33. Savitsky, D., Ward, B.P. (1976). Procedures for Hydrodynamic Evaluation of Planing Hulls in Smooth and Rough Water. Marine Technology and Sname News, vol. 13, no. 4, 381-400, DOI: -
34. Huang, S., Jiao, J., Chen, C. (2021). CFD prediction of ship seakeeping behavior in bi-directional cross wave compared with in uni-directional regular wave. Applied Ocean Research, vol. 107, 102426, DOI: 10.1016/j.apor.2020.102426
35. Nimma, R.B., Arundeepan, V., Shashikala, A.P. (2018). Ship Motion in Viscous Flow under Irregular Waves. International Journal of Scientific & Engineering Research, vol. 9, no. 4, 8-13, DOI: -
36. Bhattacharya, R. (1978). Dynamics of Marine Vehicles. John Wiley & Sons, New York.
37. Lewkowicz, R. (2019). A centrifuge-based flight simulator: Optimization of a baseline acceleration profile based on the motion sickness incidence. Acta Astronautica, vol. 164, 23-33, DOI: 10.1016/j.actaastro.2019.07.007
38. Cepowski, T. (2012). The prediction of the Motion Sickness Incidence index at the initial design stage. Zeszyty Naukowe, vol. 31, 45-48, DOI: -

Paper submitted: 29.12.2021.
Paper accepted: 23.04.2022.